Supplementary Information

Tailoring phase transition pathway of Ag_2Te nanowires via surface confinement: an in situ transmission electron microscopy study

Lei Shangguan[1,2], Ming-Yuan Wang[3], Hui-Jun Liang[4], Shuang-Ying Lei[2], Zhi-Qun Cheng[1], Long-Bing He[2,5*], and Li-Tao Sun[2,5]*

[1] School of Integrated Circuits, Nanjing University of Information Science and Technology, Nanjing 210044, P. R. China.

[2] SEU-FEI Nano-Pico Center, Key Laboratory of MEMS of Ministry of Education, Southeast University, Nanjing 210096, P. R. China.

[3] School of Mechanical Engineering, Jiangsu University, Zhenjiang 212013, P. R. China.

[4] Advanced Photonics Center, School of Electronic Science and Engineering, Southeast University, Nanjing 210096, P. R. China.

[5] Centre for Advanced Materials and Manufacture, Joint Research Institute of Southeast University and Monash University, Suzhou 215123, P. R. China.

*Corresponding Email: l.shangguan@nuist.edu.cn; helongbing@seu.edu.cn

The diameter distribution of the as-synthesized Ag_2Te nanowires is presented in Figure S1a. Statistical analysis reveals a relatively uniform distribution, with diameters predominantly ranging from 10 nm to 16 nm. This narrow size dispersion indicates good uniformity in the sample morphology, which is crucial for consistent behavior in subsequent phase transition experiments.

To characterize the carbon shell on the surface of Ag_2Te nanowires, the Ag_2Te nanowires were transferred onto pure Au grids (instead of holey carbon grids) to eliminate the strong background carbon signal from the support film. By retaining more surface hydrocarbons and applying controlled electron-beam irradiation, a more distinct and thicker carbon shell was formed, as shown in Figure S1b.

Figure S1c shows the EDS result of the as-prepared Ag_2Te nanowires, with the corresponding elemental composition listed in Table S1. The signals of Cu and C originate from the copper grid and carbon film, respectively. The atomic fractions of Ag and Te are 7.75% and 3.90%, yielding an Ag:Te atomic ratio of approximately 2:1, which confirms the composition of the nanowires as Ag_2Te.

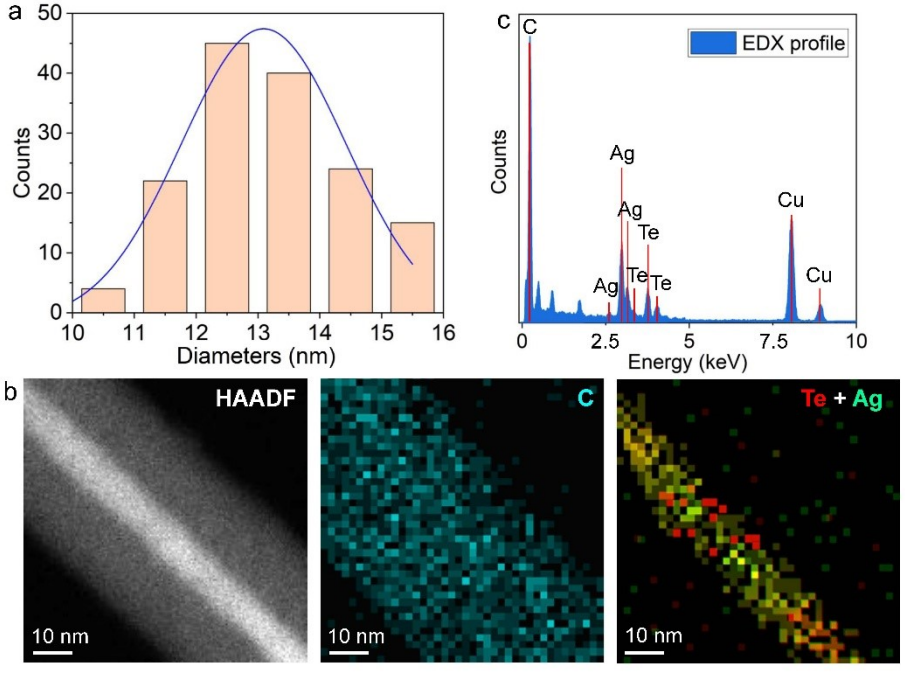

Figure S1. Characterization of the as-prepared Ag_2Te nanowires and the carbon shell. (a) Dimension distribution histogram. (b) EDS elemental mapping of the carbon shell. (c) EDS analysis results of Ag_2Te nanowires.

Table S1. Atomic fractions obtained from the EDS result in Figure S1.

Elements	Atomic fraction (%)
C	68.03
Cu	20.32
Ag	7.75
Te	3.90

Figure S2a shows the HRTEM image of the resulted Ag_5Te_3 nanowire after phase transition. The inset shows the corresponding FFT image, which is indexed to the hexagonal Ag_5Te_3. Figure S2b shows the EDS result of this nanowire, and the corresponding atomic fractions are listed in Table S2. The atomic ratio of Ag:Te is calculated to be approximately 5:3, further confirming the formation of Ag_5Te_3.

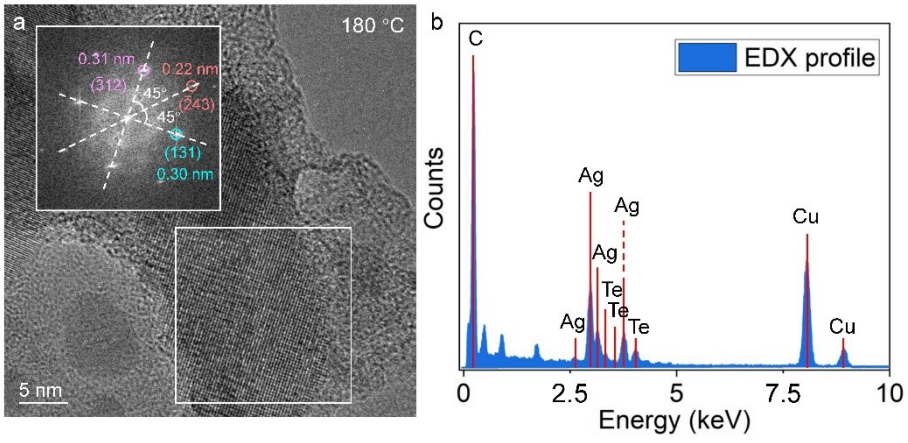

Figure S2. Characterization of the Ag_5Te_3 nanowire after phase transition. (a) HRTEM image and (b) the corresponding EDS result of the Ag_5Te_3 nanowire.

Table S2. Atomic fractions obtained from the EDS result in Figure S2

Elements	Atomic fraction (%)
C	23.73
Cu	37.53
Ag	24.25
Te	14.48

Figure S3 a-b and c-d show the HRTEM images of the Ag_2Te and Te phases (of the nanowire in Figure 3a) before and after phase transition, respectively.

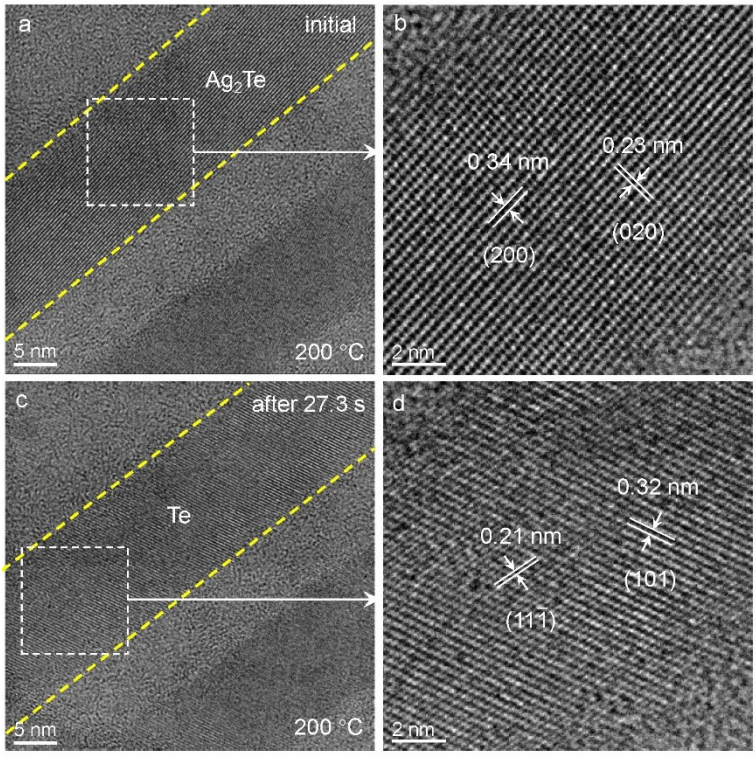

Figure S3. Phase transition from monoclinic Ag_2Te to hexagonal Te. (a-b) HRTEM image of the initial Ag_2Te nanowire. (c-d) HRTEM image of the Te nanowire after complete phase transition.

Figure S4 shows the phase transition of another Ag_2Te nanowire into Te. Notably, the entire phase transition process is rapid, completing in only 5.1 s, which prevents the capture of the moving Ag_2Te-Te interface. However, the phase transition process could be confirmed by the HRTEM and FFT images. In the FFT image shown in Figure S4a, characteristic planes belonging to the monoclinic Ag_2Te phase, such as ($\bar{1}01$) and ($\bar{1}23$), can be clearly observed. After 2.1 s, a new set of crystal planes appears, which are indexed as the (110) plane of hexagonal Te. Concurrently, the diffraction spots of the Ag_2Te ($\bar{1}23$) plane also split, leading to the emergence of the Te ($\bar{1}1\bar{2}$) plane (Figure S4b). After 5.1 s, the diffraction spots corresponding to the monoclinic Ag_2Te phase completely disappears (Figure S4c). The emerged diffraction spots could be indexed to the (110), (01$\bar{1}$), ($\bar{1}1\bar{2}$), and ($\bar{1}0\bar{1}$) planes of hexagonal Te, indicating a complete phase transition into hexagonal Te. The HRTEM image of the nanowire in Figure S4d also clearly shows the lattice fringes of the (01$\bar{1}$) and ($\bar{1}1\bar{2}$) planes in the Te crystal.

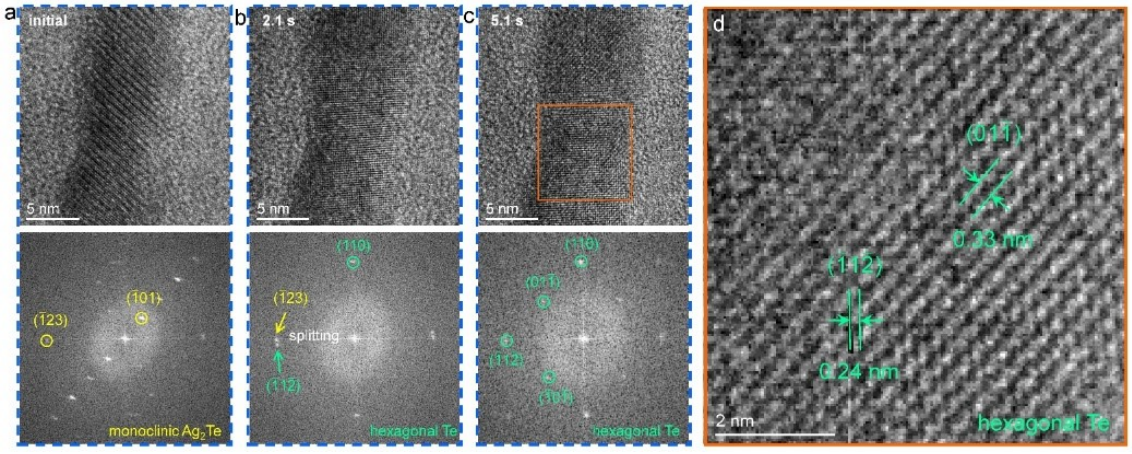

Figure S4. Phase transition of an Ag_2Te into Te. TEM images and the corresponding FFT patterns of the nanowire at (a) the initial state, (b) 2.1 s, and (c) 5.1 s. (d) HRTEM image corresponding to the orange-boxed region in (c).

Figure S5 shows the HRTEM images and EDS mappings of the Ag_2Te-Te interface acquired during phase transition from monoclinic Ag_2Te to hexagonal Te.

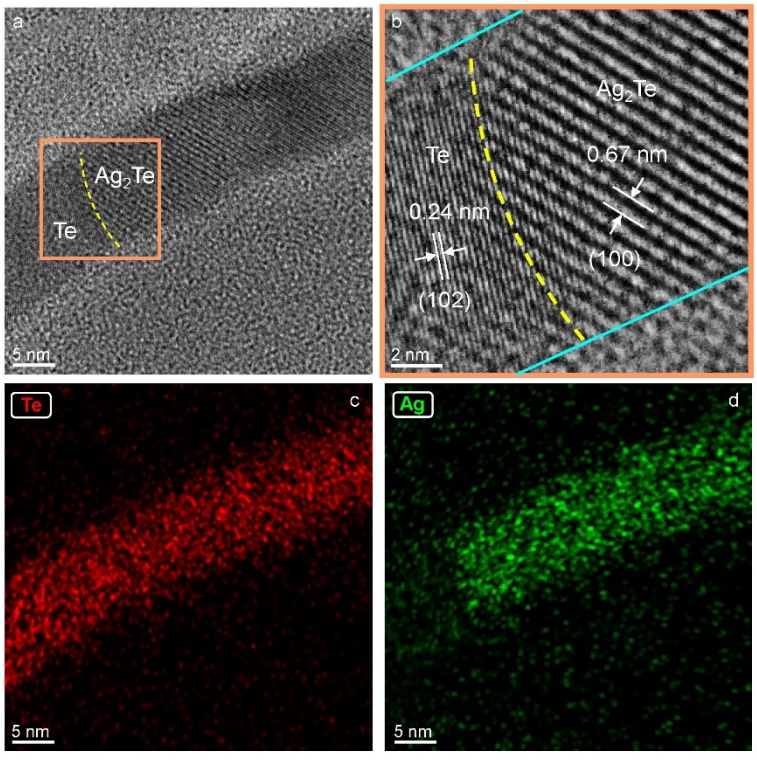

Figure S5. Characterization of the Ag_2Te-Te interface during phase transition. (a-b) HRTEM images and (c-d) EDS mappings of the Ag_2Te-Te interface.

As shown in Figure S6, the region encapsulated by the carbon shell remains smooth and particle-free, whereas the exposed region exhibits pronounced Ag surface diffusion and subsequent nanoparticle formation, highlighting the effective confinement role of the carbon shell.

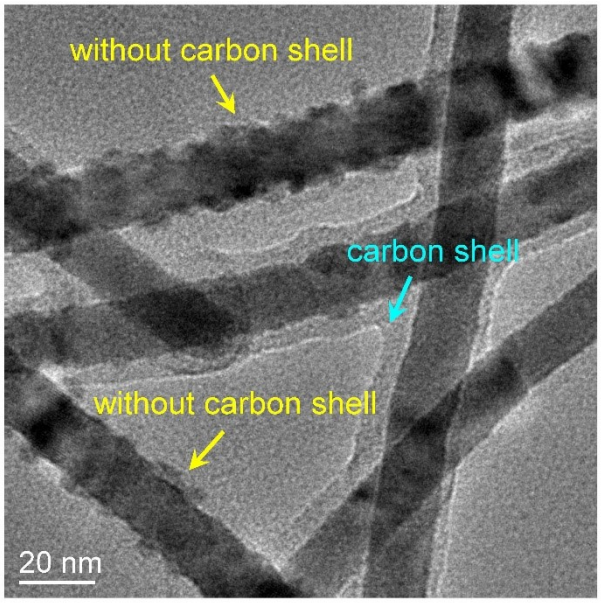

Figure S6. Surface diffusion contrast between carbon-encapsulated and exposed regions of the Ag_2Te nanowires.

Figure S7 shows the diffusion of the Ag nanoparticles from an Ag_2Te nanowire with free surface, causing the disappearance of diffraction spots.

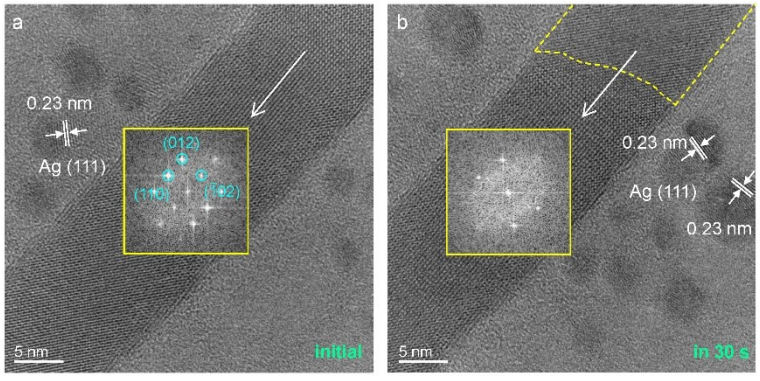

Figure S7. Diffusion of the Ag nanoparticles from the Ag_2Te nanowire with free surface. HRTEM images of this Ag_2Te nanowire (a) before and (b) after Ag diffusion, respectively.

As shown in Figure S8, at 200 °C, the mobilized Ag atoms no longer form discrete nanoparticles on the surface but instead undergo large-scale aggregation, coalescing into bulk Ag clusters at nanowire junctions, which is directly correlated with the complete phase transition from Ag_2Te to Te.

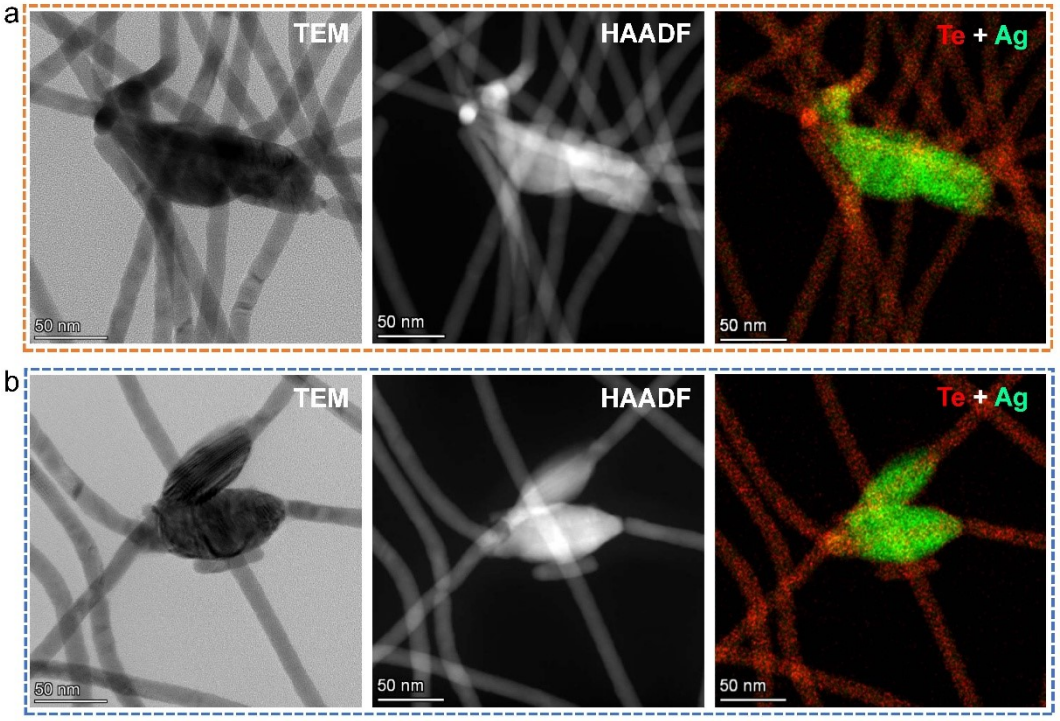

Figure S8. Aggregation of Ag at nanowire junctions during phase transition from Ag_2Te to Te.